ELSEVIER

Journal of Power Sources 105 (2002) 151–160

JOURNAL OF POWER SOURCES

www.elsevier.com/locate/jpowsour

Anodic materials for rechargeable Li-batteries

Mario Wachtler*, Martin Winter, Jürgen O. Besenhard

Institute for Chemical Technology of Inorganic Materials, Graz University of Technology, Stremayrgasse 16, 8010 Graz, Austria

Abstract

Six sub-micro-crystalline alloy powders (Sn–Sb, Sn–Ag, Sb–Ag, and Sn–Sb–Ag alloys), where all constituents are able to alloy reversibly with Li and which are therefore characterized by large theoretical Li storage capacities, have been synthesized by chemical precipitation with $NaBH_4$, and their composite electrodes have been electrochemically tested by constant current cycling and cyclic voltammetry. Sn/SnSb and SnSb showed the best performance, with stable capacities of 600 and 500 mAh g^{-1}, respectively, for more than 30 cycles. All of the materials exhibit large irreversible capacities in the first cycle, which are also often found for other metallic–intermetallic systems. Since, however, first cycle efficiencies of 89–95% can be achieved with electroplated thin Sn films, this is not an intrinsic problem of Sn or Sn-containing compounds, and it is not the trapping of Li in any of the many lithiated Sn phases that should be the main reason for the large irreversible capacities of the composite electrodes, but rather other factors, such as oxide impurities and especially contact problems in the composite electrode.

Keywords: Li storage alloys; Sn–Sb, Ag–Sn, Ag–Sb, Ag–Sb–Sn alloys; First cycle irreversible capacity; Trapping of Li; $NaBH_4$ (borohydride) process

1. Introduction

Among the many materials which have been proposed as anodes for Li-ion batteries, metals such as Al, Sn, Si, etc. are a special case. On the one hand, they exhibit enormous theoretical Li storage capacities, on the other hand they suffer from insufficient long-term cycling stability due to the large volume changes which occur during lithiation and de-lithiation. It has been demonstrated by the various research groups that these shortcomings can (partly) be overcome for instance by reducing the particle size of the host material, by using multi-phase instead of single-phase materials, or by using intermetallic compounds (alloys) (cf., e.g. [1] and the references therein). Many of the intermetallic compounds of the above-mentioned metals exhibit similar or smaller Li storage capacities than the pure metals, but often show an increased long-term cycling stability. In analogy to the hydrogen storage metals/alloys in metal hydride batteries, they may be called lithium storage metals/alloys.

In principle, there are three ways how an intermetallic compound can react with Li.

1. It inserts Li in a topotactic reaction:

$$x\mathrm{Li} + \mathrm{MM}'_y \leftrightarrow \mathrm{Li}_x\mathrm{MM}'_y$$

Topotactic reactions are usually limited to the accommodation of small amounts of Li, as the available empty interstitial sites in the host are limited. Therefore, the Li storage capacities are low. On the other hand, since no significant changes occur in the structure of the host material and since volume changes are usually small, the cycling stabilities are very good. If further Li is inserted, the crystal structure rearranges and alloying reactions occur. An example is Cu_6Sn_5 [3,4] which in a first step forms a structurally related Li_2CuSn-type phase. When further Li is inserted, the ternary phase decomposes into Cu and Li_xSn alloys. Topotactic reactions have also been proposed for Mg_2Si [5] and InSb [6]. However, for InSb, the range of topotactic insertion is limited to the very initial stage, and is soon followed by a displacement of In from the Sb lattice and the formation of Li_3Sb (or $Li_{x+y}In_{1-y}Sb$) and Li_zIn [6,7].

2. One (the active) component of the intermetallic alloys with Li while the other is displaced from the original lattice; the displaced component does not alloy with Li:

$$x\mathrm{Li} + \mathrm{MM}'_y \leftrightarrow \mathrm{Li}_x\mathrm{M} + y\mathrm{M}'$$

or if the displacement is irreversible:

$$x\mathrm{Li} + \mathrm{MM}'_y \rightarrow \mathrm{Li}_x\mathrm{M} + y\mathrm{M}' \leftrightarrow x\mathrm{Li} + \mathrm{M} + y\mathrm{M}'$$

As a result, a finely inter-dispersed composite of a lithiated phase in an unreacted (non-lithiated) matrix is

* Corresponding author.
E-mail address: wachtler@ictas.tu-graz.ac.at (M. Wachtler).

0378-7753/02/$ – see front matter
PII: S0378-7753(01)00934-X

obtained, i.e. a further nano-structuring occurs in situ during charge. Examples are Sn_2Fe [8], Ni_xSn [9,10], Cu_6Sn_5 (at high lithiation states) [3,4], a number of other M_2M' alloys with M = Sn, Ge, or Sb [11], NiSi and FeSi [12], or Mg_xNi [13]. The presence of the inactive component reduces the theoretical specific charges and charge densities compared to the pure active metals. On the other hand, the presence of a non-reactive phase stabilizes the composite material, as the volume expansion of the overall electrode material is decreased (the active phase is "diluted"), and as the inactive matrix can "buffer" the volume changes of the active phase. In the case of Sn, it also serves as barrier against the aggregation of Sn into larger grains, which has been identified as one of the reasons for the declining capacities of Sn-based anode materials during long-term cycling [14].

3. One component of the intermetallic alloys with Li with a concomitant displacement of the other from the original lattice; the displaced component then also alloys with Li:

$$(x+y)\mathrm{Li} + \mathrm{MM}'_z \leftrightarrow y\mathrm{Li} + \mathrm{Li}_x\mathrm{M} + z\mathrm{M}' \leftrightarrow \mathrm{Li}_x\mathrm{M} + z\mathrm{Li}_{y/z}\mathrm{M}'$$

As a result, a composite of two finely interdispersed lithiated phases is obtained. Examples are SnSb [2,15–17] and InSb (at higher lithiation states) [6,7]. Since both components react with Li, the theoretical Li storage capacities are in the range of those of the pure metals and in any case larger than for intermetallics from group (2). Concerning the cycling stability, also here a certain "buffer" effect should be given, as the components react one after each other and the non-reacting phase can buffer the reacting phase. Besides, the active matrix should retard the aggregation of Sn as an inactive matrix does. The volume changes of the overall electrode material are, however, larger than above.

Generally, the borders between the various ways of reaction are floating and the actual reaction products may depend to some extent on electrochemical parameters such as the cut-off potential and the charging rates, but also on the specific morphology of the starting material, or the presence of dopants, etc. What has not been considered above is the reversibility of the reactions. Whereas, for example, for SnSb, it has been demonstrated that the displacement of Sn from the Sb lattice is highly reversible,[1] for NiSi and FeSi, it is believed that the extrusion of Fe and Ni from the Si lattice is almost irreversible [12].

At the moment, the most frequently used method to synthesize such alloy powders seems to be mechanical alloying by ball-milling. An interesting alternative is a reductive precipitation process with $NaBH_4$, which has been adopted here. The particle size and morphology of the precipitate can thereby be influenced by the precipitation conditions, such as concentrations, temperature and especially by the presence of suitable complexing agents, and ultrafine powders can easily be obtained. Furthermore, when more than one reducible metal species are present in the starting solution, intermetallic compounds are accessible. In principle, reduction with $NaBH_4$ can be carried out both in aqueous and organic solutions, and is thus a powerful tool in materials chemistry. Some interesting applications include, e.g. the preparation of metal/ceramic composites [18], transition metal oxides as cathode materials for lithium batteries [19], or amorphous nano-crystalline alloys for hydrogen storage in Ni–metal hydride batteries [20].

The excellent electrochemical performance of Sn/SnSb alloy powders has already been demonstrated in previous works [2,17]. Here, the investigations are extended to other multi-phase, multi-component materials from the ternary system Ag–Sb–Sn, of which all three constituents are active towards Li. As recently re-investigated by Oberndorff et al. [21], the ternary system Ag–Sb–Sn exhibits a number of binary intermetallic compounds such as Sn_4Sb_3, Sn_3Sb_4, $SnAg_3$, $SnAg_4$, $SbAg_3$, and $SbAg_4$. Apart from mutual solubility of the elements in the other phases, which holds especially true for the isomorphous compounds $SnAg_4$ and $SbAg_4$ thus forming (Sn, Sb)Ag_4, no ordered ternary intermetallic phases have been found.

The six materials under investigation are in detail: three Sn–Sb alloys (with the compositions Sn/SnSb,[2] SnSb, Sb/SnSb), an Ag–Sn alloy (Sn/$SnAg_{3-4}$), an Ag–Sb alloy (Sb/$SbAg_{3-4}$), and an Ag–Sb–Sn alloy (Ag/SnSb/$SnAg_{3-4}$/$SbAg_{3-4}$[3]).

Finally, the large irreversible capacities in the first cycle of these materials are compared to those of electroplated thin films of pure Sn and discussed with special regard to possible trapping of Li.

2. Experimental

2.1. Alloy powders and composite electrodes

The multi-phase alloy powders and Ni powder were synthesized by precipitation with $NaBH_4$ in aqueous solutions. Therefore, a $NaBH_4$-solution was rapidly added to a solution of the appropriate metal-precursors (usually chloride salts, except in the case of the Ag-containing powders) under strong stirring, as has been described in detail in [2]. For the Ag-containing powders, a separate Ag^+-solution was prepared and added to the Sn^{2+}/Sb^{3+}-solution simulta-

[1] In the long run, however, the material gets increasingly amorphous and at large cycle numbers the SnSb phase gradually disappears [15].

[2] See [21,2] for problems related with the exact stoichiometry of the phase "SnSb".

[3] The phases $SnAg_3$, $SnAg_4$, $SbAg_3$, and $SbAg_4$ have very similar structures and are difficult to distinguish by X-ray diffraction. Therefore, and because of mutual solubility, the phase assignment of the ternary alloy should not be taken too literally.

neously with the $NaBH_4$-solution to avoid the precipitation of metallic Ag according to the reaction: $Sn^{2+} + 2Ag^{+} \rightarrow Sn^{4+} + 2Ag^{0}\downarrow$. In this way, the formation of metallic Ag could probably not be totally excluded, but a distinct Ag phase could only be detected in the Ag–Sb–Sn alloy.

The BET surface areas of the powders obtained were in the range of 10–50 $m^2\,g^{-1}$ (which corresponds to average particle diameters of around 15–70 nm—assuming ideal spherical shape of the particles and using the crystallographic densities for the calculation). The crystallographic compositions of the powders have been determined with X-ray powder diffraction (XRD).

Composite electrodes were prepared by painting a slurry of 82 wt.% alloy powder, 10% Ni (acting as electronically conductive additive), and 8% poly(vinylidene fluoride) (PVdF) (Aldrich, $M_w = 534{,}000$), suspended in decane (Aldrich, ≥99%), onto both sides of a stainless steel mesh of wire diameter 25 μm and mesh width 67 μm (mesh 280), serving as current collector. Then 2.1–2.3 mg of composite material were brought up on a geometric area of 2 sides ×4 mm × 4 mm. Before usage, the composite electrodes were pressed and rigorously dried under dynamic medium-high vacuum [2].

2.2. Electroplated Sn electrodes

Thin porous Sn films were electroplated onto Cu-substrates from an aqueous solution containing 36 g l^{-1} $Sn_2P_2O_7$ (Merck, p.a.), 135 g l^{-1} $K_4P_2O_7$ (Merck, p.a.), and 0.3 g l^{-1} gelatine (Fluka, medium gel strength, 180 bloom) at current densities of 2.5 mA cm^{-2}, at room temperature, without stirring, and with a Sn-rod as counter electrode [15]. The Sn films covered a geometric area of 81 mm^2 and were a few microns thick.

2.3. Constant current cycling and cycling voltammetry

The electrochemical experiments were performed in laboratory-type glass cells with metallic Li as counter and reference electrodes and with an excess of electrolyte. The working electrodes were not closely packed in separator materials but loosely placed in the electrolyte without further support or protection.

The alloy powder composite electrodes were cycled in 1 mol l^{-1} $LiPF_6$/ethylene carbonate (EC)–diethyl carbonate (DEC) (1:1) (Mitsubishi Chemical Corp., Sol-Rite®), between 20 and 1200 mV, using a current density of 0.5 mA cm^{-2} (with respect to the geometric electrode area), which corresponds to specific currents between 84.8 and 92.9 mA $g(AM)^{-1}$ (with respect to the mass of active material, AM).

The electroplated Sn electrodes were cycled in 1 mol l^{-1} $LiClO_4$ (Merck, Selectipur®)/propylene carbonate (PC) (Merck, Selectipur®), between 20 and 1200 mV, using current densities of 0.02–0.5 mA cm^{-2}. Between charge and discharge, the cycling was interrupted for 5 min and the open circuit voltage (OCV) was monitored to get a rough estimation of the electrode polarization.

The terms ''charge'' and ''discharge'' refer to the alloy/Sn electrodes being used as anodes in full Li-ion cells (though in the present half-cell studies they are used as cathodes), i.e. to Li insertion and de-insertion, respectively. The coulombic efficiencies are defined as Li de-insertion (discharge) capacity divided by Li insertion (charge) capacity. All potentials are given versus Li/Li^+.

Cyclic voltammograms (CVs) have been recorded in 1 mol l^{-1} $LiPF_6$/EC–DEC (1:1) between ~2700 (OCV of the uncharged electrodes) and 20 mV with scan rates of 20 μV s^{-1}.

3. Results and discussion

The electrochemical behaviors of the composite electrodes with the three Sn–Sb alloys are shown in Fig. 1 (constant current cycling) and Fig. 2 (cyclic voltammetry). Of the new materials, SnSb shows the best capacities capacities (~500 mAh g^{-1}), which are almost in the order of those of Sn/SnSb (~600 mAh g^{-1}) that have been previously reported [17]. Compared to results with electroplated Sn/SnSb materials [15], the plateaux in the charge/discharge profiles of the constant current cycling tests and the peaks in the CVs are poorer resolved, which renders an exact interpretation more difficult. Nevertheless, some interesting features can be noticed. For all materials (also for the Ag-containing alloys), the first cycle differs from the next ones, i.e. the materials undergo a formation cycle in which—among other factors—the first expansion of the active material and the composite electrode occurs [15,22]. This is especially pronounced for the Sn/SnSb electrodes, where voltage spikes are found, which are attributed to a local break-up of the composite material and sudden access of the electrolyte to the electrode interior (also cf. [22,23]). In the CVs of the Sn/SnSb and SnSb alloys, five peaks are observed during the cathodic and the anodic scans, which are ascribed to the reaction of the phase SnSb to Li_3Sb and Sn according to a mechanism: $SnSb + 3Li^+ + 3e^- \leftrightarrow Li_3Sb + Sn$ (peaks A and A′)[4], and the reaction of Sn to various lithiated Sn-phases (e.g. [14]) (B–E, B′–E′). The presence of the peaks B–E (B′–E′) in the pure SnSb material (without an excess Sn phase) is a further indication of the above reaction mechanism of SnSb. Especially, for the SnSb and Sb/SnSb materials the peak A′ exhibits a shoulder at the lower potential side, which might indicate that the reaction occurs in two steps. However, an intermediate product such as Li_2Sb [24,25], could not be detected by XRD so far, neither for pure Sb hosts nor for Sn–Sb alloys.

The cycling stability of the Sb/SnSb material is rather poor compared to the other materials. The CV is dominated by the reactions of Sb and SnSb, which occur almost at the

[4] Residual amounts of Sn can be present in the Li_3Sb lattice.

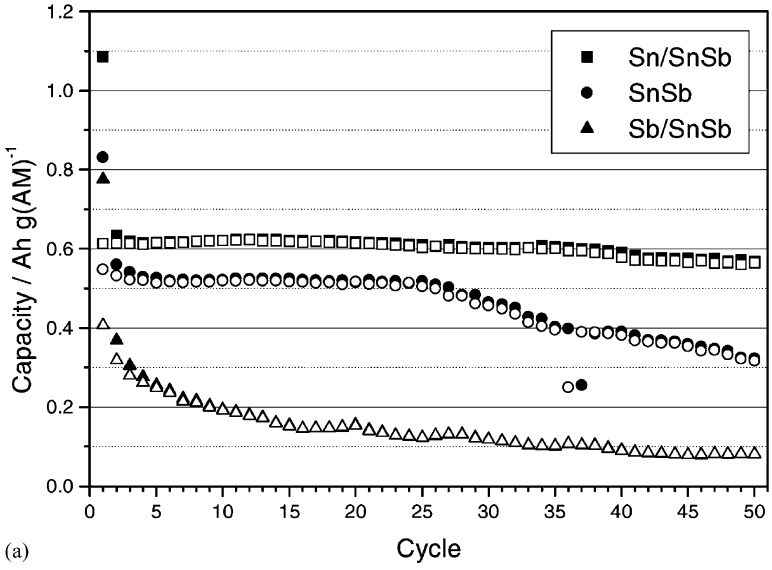

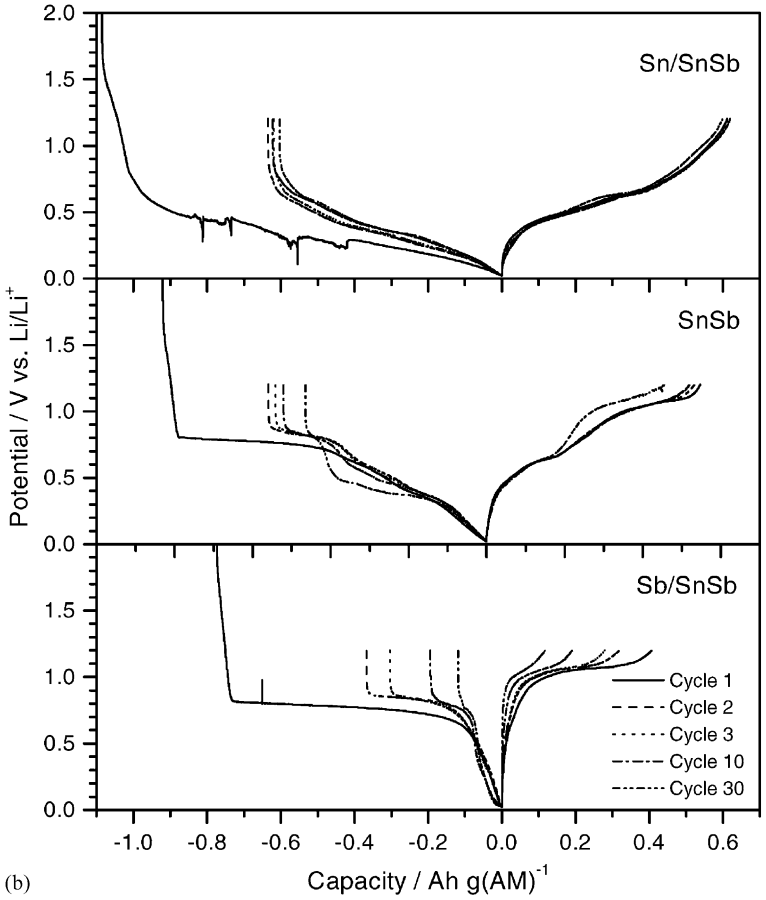

Fig. 1. Constant current cycling tests of composite electrodes with Sn–Sb alloys: (a) charge (closed symbols) and discharge (open symbols) capacities; (b) charge/discharge profiles for selected cycles.

same potential. The formation of Li_xSn phases is only faintly observed. Also a comparison of the lengths of the plateaux associated with the formation of Li_3Sb phases (~700–800 mV at the present current rates) and of the Li_xSn phases (lower potentials) during constant current cycling shows that only a minor amount of the total reversible capacity is associated with Sn, and that less Sn has reacted than would have been expected from the composition. The origin of the additional small peaks in the second and third anodic scan indicated with an asterisk is not clear at the moment.

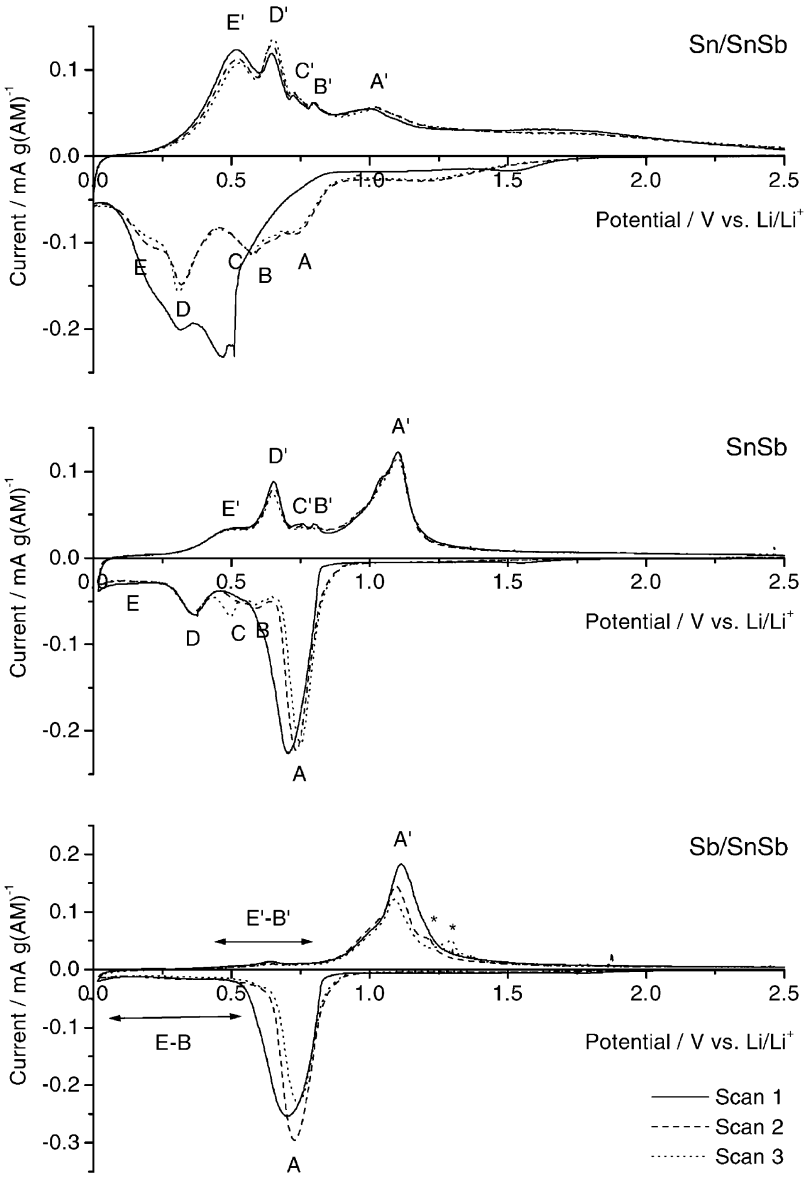

Fig. 2. Cyclic voltammograms of composite electrodes with Sn–Sb alloys.

Also the cycling performances of the Ag-containing materials (Fig. 3) are worse than those of the Sn/SnSb and the SnSb materials, though with ∼200–350 mAh g^{-1}, their capacities are still higher than for other intermetallic materials such as Cu_6Sn_5 [3]. However, the results for the Ag-containing materials are only of preliminary nature, and a thorough optimization of the composite electrodes as for the Sn–Sb alloy composite electrodes has not been undertaken. In the CVs of the Sn/$SnAg_{3–4}$ and Sb/$SbAg_{3–4}$ materials (Fig. 4), the peaks which are due to the reactions of Sn (B′–E′) and Sb (A′) are clearly visible. The additional peaks (A′ and F′ for Sn/$SnAg_{3–4}$, C′ and B′ for Sb/$SbAg_{3–4}$) are consistent with those found for the lithiation of pure Ag (in the case of Sn/$SnAg_{3–4}$, some of them are masked by peaks from Sn). As may be seen from constant current cycling tests [16] or from the CV in Fig. 5, Ag starts to react at potentials of ∼100 mV.[5] For the cathodic scan at least two peaks (B and C) and for the anodic scan at least three peaks (B′–D′) are observed, which points at a multi-step alloying mechanism. In fact, several phases Li_xAg have been described [24,26]. Whether the small peak at higher potentials (A and A′) is due to the reaction of Ag or to an impurity phase cannot be said. It is, however, also observed in the CVs of the Ag-containing alloys in Fig. 4. Based on a comparison of the CVs of Ag-containing alloys and pure Ag, it seems likely that during lithiation, the constituent com-

[5] Please note that the first scan was reversed at 0 mV, whereas the second and third were reversed at 20 mV. The strong difference in the intensities of peak D indicates that significant amounts of Li can be stored below 20 mV, which, however, in view of an application in commercial two-electrode cells is probably too close to the potential of the deposition of metallic Li.

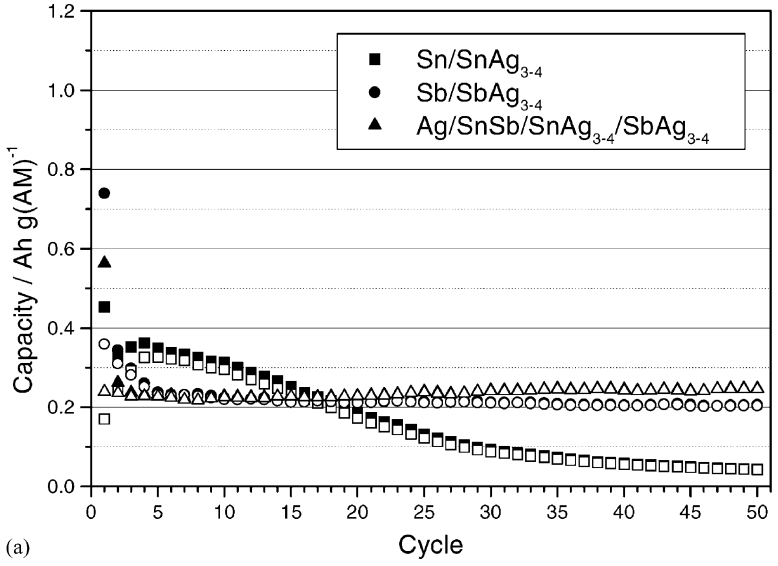

(a)

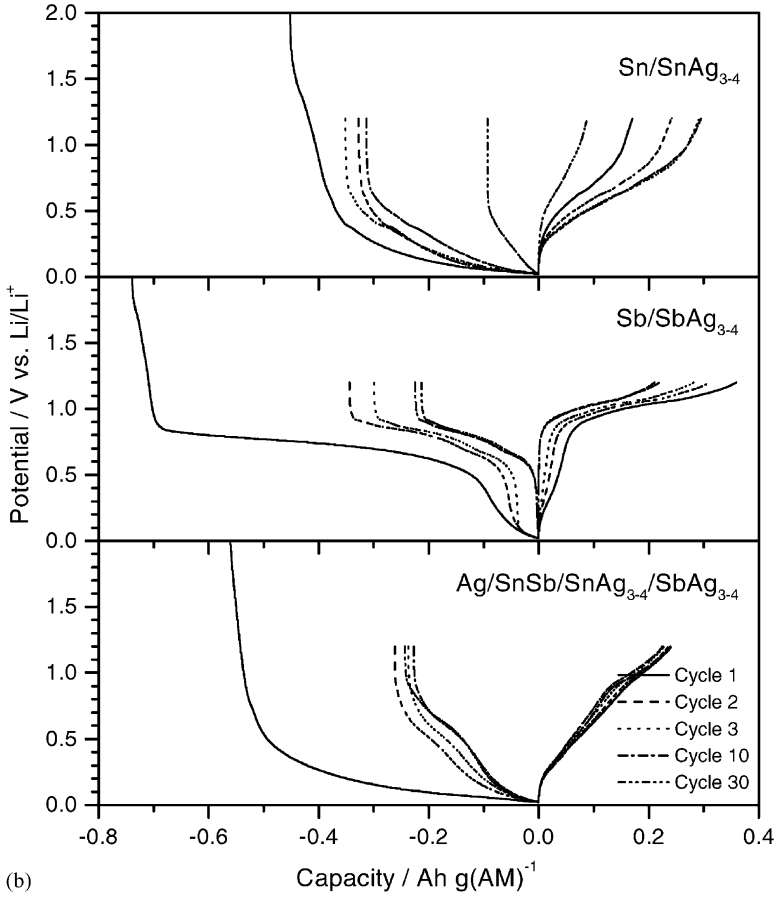

(b)

Fig. 3. Constant current cycling tests of composite electrodes with Ag-containing alloys: (a) charge (closed symbols) and discharge (open symbols) capacities; (b) charge/discharge profiles for selected cycles.

ponents of $SnAg_{3–4}$ and $SbAg_{3–4}$ segregate and form separate alloys with Li, like in the case of SnSb. However, for a final proof and an unequivocal assignment of the various reactions and the intermediate and final lithiated phases X-ray diffraction investigations are inevitable.

Common to all six investigated materials is the low coulombic efficiency in the first charge/discharge cycle (e.g. 50–65% for the Sn–Sb alloys). As has already been shortly addressed in previous works [2,17], this is ascribed to essentially four effects.

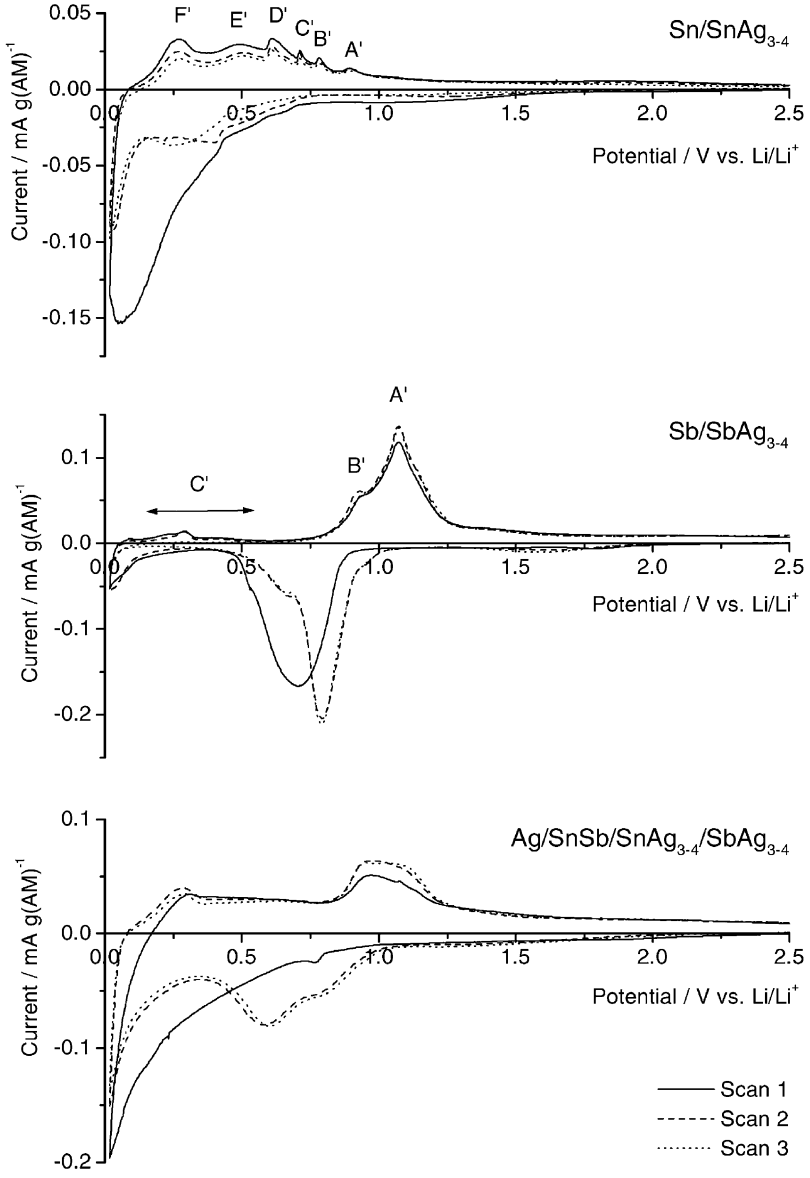

Fig. 4. Cyclic voltammograms of composite electrodes with Ag-containing alloys.

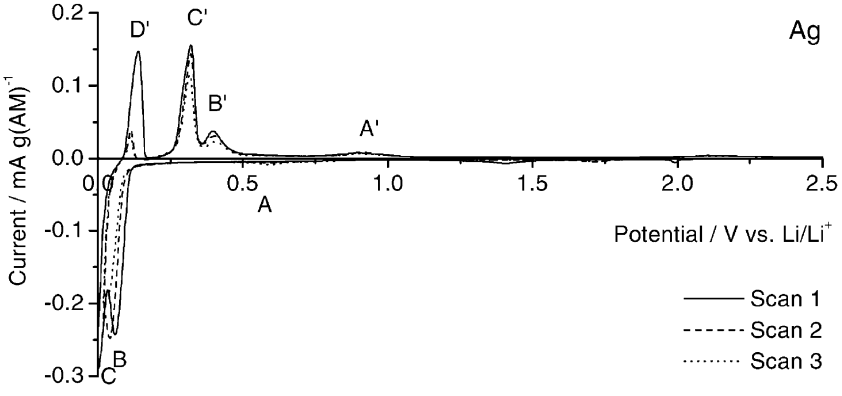

Fig. 5. Cyclic voltammogram of a Ag composite electrode.

1. *Electrolyte decomposition at the electrode/electrolyte interphase and the formation of a protective film*. These corrosive reactions cannot be totally prevented, however, it should be possible to minimize them by a careful choice of the electrolyte components and by the addition of suitable reactive electrolyte additives, which allow the fast formation of dense, flexible films, or of surfactant electrolyte additives, which retard film-formation [17,23].
2. *Reduction of oxide impurities*. Due to the preparation method the alloy powders (especially those with Sn) and the Ni powder contain oxide impurities, which are irreversibly reduced to the respective metals and Li_2O during the first charge. Newer experiments have shown that these oxides can be partly removed by washing the freshly precipitated powder in alkaline solution or in solutions of selected complexing agents.
3. *Loss of contact*. The enormous volume changes which the active material undergoes during Li uptake and release are the cause for strong mechanical strain which can lead to cracking and disconnection of parts of the active material, which are then lost for the cycling process. Besides, these volume changes are the source of strong dispersive forces in the composite electrode which have to be counteracted by the binder. Both the binding strength and the electrolyte uptake behavior of the binder (which in turn influences the binding strength), are determined by the chemistry of the binder but also by its physical distribution within the composite electrode [22,23].
4. *Trapping of lithium*. Finally, there is a number of thermodynamic and kinetic reasons, why not all of the inserted Li can be re-extracted, such as immobilization of Li at structural or electronic defect sites, a rest-solubility of Li in the host material at the applied discharge cut-off potential, slow Li diffusion rates, slow lithiation and de-lithiation reaction rates, the presence of kinetic barriers, etc. Another point is the partial disconnection of a host particle with the consequence that de-lithiation has to proceed through a bottle neck and the diffusion paths get longer. In the case of Sn, the situation is aggravated by the fact that a large number of intermetallic phases Li_xSn exist, which during charge (or discharge) are formed subsequently. Hence many reactions occur one after the other (or in other words: many reaction zones move through the active material), whereas for instance for Al or Sb only one reaction occurs.[6] Therefore, the opportunities to trap Li in one of the many lithiated phases of Sn are more than for the other metals.

A comparison with other systems which have been reported in the literature shows that the large irreversible capacity in the first cycle is not a unique feature of the present Li storage alloys, but that it is found for many Sn-containing systems. Therefore, the question arises whether it is an intrinsic property of Sn (as outlined in point (4)), which cannot be influenced, or whether it is only a result of the present specific structure and morphology of the active material or the present design of the composite electrode. To answer this question, porous Sn films of a few microns thickness have been prepared by electroplating and their cycling behavior in the first cycle has been studied (Fig. 6). The electroplated host has been chosen to exclude effects from the composite electrode which might also result in a poor contact already in the beginning or in a gradual loss of contact during cycling, e.g. due to swelling of the binder.

With a discharge cut-off potential of 1200 mV and current densities of 0.1 mA cm^{-2} and below,[7] coulombic efficiencies of 94–95% are obtained (Fig. 6b). As the current density is increased, the efficiency drops to, e.g. 89–90% for 0.5 mA cm^{-2}. Hence, in principle, it is possible to achieve high efficiencies with Sn already in the first cycle, and it is not the trapping of Li in any of the Li_xSn phases that seems to be the major reason for the large irreversible capacities, but the other points, especially the reduction of oxide impurities and loss of contact.

Apart from the decreasing efficiencies (above 0.1 mA cm^{-2}), it is observed that with increasing current density the capacities decrease, as the electrode overpotential increases and the charge cut-off potential is reached earlier (cf. the inset in Fig. 6a, displaying the evolution of the OCV during the 5 min where the current has been switched off after charge). Besides, it is interesting to note that the charge profiles for the first cycle differ for the different current densities. At 0.02 mA cm^{-2}, three potential plateaux are observed, which can be ascribed to the formation of Li_2Sn_5 (at ~675 mV), LiSn (~575 mV), and higher-lithiated phases Li_7Sn_3–$Li_{22}Sn_5$ (~450 mV, including the shoulder beginning at ~370 mV). As the current density is increased, the formation of the two phases Li_2Sn_5 and LiSn is partly (0.05 and 0.1 mA cm^{-2}) or fully (0.2 and 0.5 mA cm^{-2}) suppressed. It is obviously a kinetic effect, which has also been observed with coarse-grained Sn matrices, and which has been attributed to the slow diffusion rates of Li in the Li-poor Li_xSn phases [16,27]. During discharge, all plateaux are observed regardless of the current densities. With a maximum reversible capacity of 700 mAh g^{-1} even for the lowest current densities only ~70% of the theoretical capacity (994 mAh g^{-1}) could be utilized. This may be explained with the charge cut-off potential of 20 mV (further lithiation is possible at lower potentials, however with the risk of the deposition of metallic Li) and loss of contact.

[6] This reasoning is somewhat simplified since it does not take into account the different volume changes (which are smaller for two neighbouring Li_xSn phases with small differences in x than for Sb/Li_3Sb) and the structural relations between the various phases (i.e. if small or severe structural rearrangements occur during lithiation/de-lithiation).

[7] This corresponds to ~115 mAh g^{-1} or a *C*/6 rate with respect to the experimentally observed capacity of ~700 mAh g^{-1}.

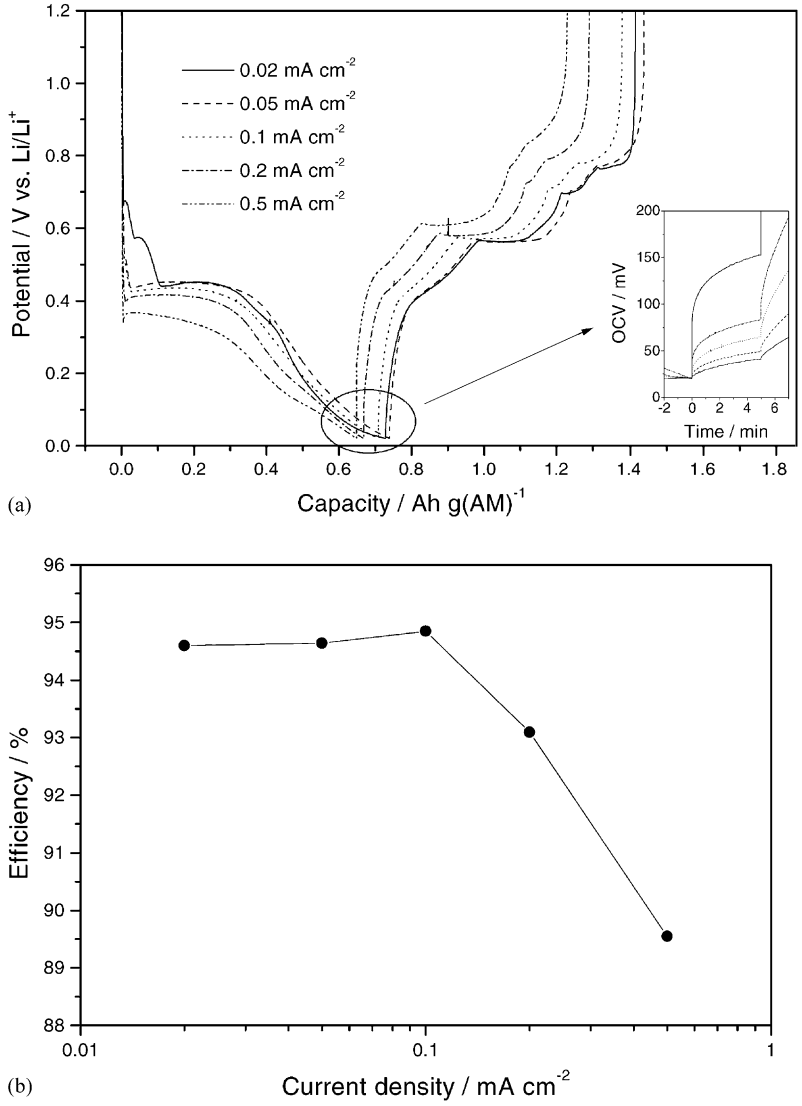

Fig. 6. Constant current charge and discharge of a thin electroplated Sn film at various current rates: (a) charge/discharge profiles; (b) coulombic efficiencies.

4. Conclusions

Composite electrodes with six different multiphase and multicomponent alloy powders from the system Ag–Sb–Sn, which have been prepared by chemical precipitation with $NaBH_4$, have been tested. Especially, the Sn/SnSb and SnSb alloy powders exhibited high capacities and good cycling stabilities. The performance of the Ag-containing materials was poorer, however these are only first results obtained with non-optimized electrodes.

Generally, it was found that the irreversible capacities in the first cycle are rather large. But this is not an intrinsic feature of Sn or Sn-containing materials in general, e.g. due to trapping of Li in any of the many Li_xSn phases, since with electroplated thin Sn films first cycle efficiencies of 89–95% could be achieved. Rather than that, it is attributed to oxide impurities in the alloy powders and especially to problems with the composite electrode (loss of contact during cycling). Hence, in principle a further improvement of the present materials should be realistic.

Acknowledgements

Financial support by the Austrian Science Fund and the Oesterreichische Nationalbank in Project 12768 and in the Special Research Program ‘‘Electroactive Materials’’ as well as support by Mitsubishi Chemical Corp. (Japan) are gratefully acknowledged. Merck (Germany) is thanked for the donation of electrolytes.

References

[1] M. Winter, J.O. Besenhard, Electrochim. Acta 45 (1999) 31.
[2] J. Yang, M. Wachtler, M. Winter, J.O. Besenhard, Electrochem. Solid State Lett. 2 (1999) 161.

[3] K.D. Kepler, J.T. Vaughey, M.M. Thackeray, Electrochem. Solid State Lett. 2 (1999) 307.
[4] D. Larcher, L.Y. Beaulieu, D.D. MacNeil, J.R. Dahn, J. Electrochem. Soc. 147 (2000) 1658.
[5] H. Kim, J. Choi, H.-J. Sohn, T. Kang, J. Electrochem. Soc. 146 (1999) 4401.
[6] C.S. Johnson, J.T. Vaughey, M.M. Thackeray, T. Sarakonsri, S.A. Hackney, L. Fransson, K. Edström, J.O. Thomas, Electrochem. Comm. 2 (2000) 595.
[7] K.C. Hewitt, L.Y. Beaulieu, J.R. Dahn, in: Proceedings of the 198th Meeting of the Electrochemical Society, Phoenix, AZ, USA, 22–27 October 2000, Abstract no. 128.
[8] O. Mao, R.L. Turner, I.A. Courtney, B.D. Fredericksen, M.I. Buckett, L.J. Krause, J.R. Dahn, Electrochem. Solid State Lett. 2 (1999) 3.
[9] O. Crosnier, T. Brousse, D.M. Schleich, Ionics 5 (1999) 311.
[10] G.M. Ehrlich, C. Durand, X. Chen, T.A. Hugener, F. Spiess, S.L. Suib, J. Electrochem. Soc. 147 (2000) 886.
[11] D. Larcher, L.Y. Beaulieu, O. Mao, A.E. George, J.R. Dahn, J. Electrochem. Soc. 147 (2000) 1703.
[12] G.X. Wang, L. Sun, D.H. Bradhurst, S. Zhong, S.X. Dou, H.K. Liu, J. Power Sources 88 (2000) 278.
[13] H. Kim, B. Park, H.-J. Sohn, T. Kang, J. Power Sources 90 (2000) 59.
[14] I.A. Courtney, J.R. Dahn, J. Electrochem. Soc. 144 (1997) 2045.
[15] J. Yang, M. Winter, J.O. Besenhard, Solid State Ionics 90 (1996) 281.
[16] J.O. Besenhard, J. Yang, M. Winter, J. Power Sources 68 (1997) 87.
[17] M. Wachtler, M. Winter, J.O. Besenhard, J. Power Sources 94 (2001) 189.
[18] L. Zhang, A. Manthiram, J. Mater. Chem. 6 (1996) 999.
[19] A. Manthiram, A. Dananjay, Y.T. Zhu, Chem. Mater. 6 (1994) 1601.
[20] M. Mitov, A. Popov, I. Dragieva, J. Appl. Electrochem. 29 (1999) 59.
[21] P.J.T.L. Oberndorff, A.A. Kodentsov, V. Vuorinen, J.K. Kivilahti, F.J.J. van Loo, Ber. Bunsenges. Phys. Chem. 102 (1998) 1231.
[22] M. Wachtler, M.R. Wagner, M. Schmied, M. Winter, J.O. Besenhard, J. Electroanal. Cham. 510 (2001) 12.
[23] J.O. Besenhard, M. Wachtler, M.R. Wagner, M. Winter, Electrochem. Soc. Proc. Ser. 2000, 32 (2001) 32.
[24] P. Villars, Pearson's Handbook, Desk Edition, Crystallographic Data for Intermetallic Phases, ASM International, 1997.
[25] R.A. Huggins, J. Power Sources 22 (1988) 341.
[26] M. Hansen, K. Anderko, Constitution of Binary Alloys, 2nd Edition, McGraw-Hill, New York, 1958.
[27] J. Yang, Y. Takeda, N. Imanishi, O. Yamamoto, J. Electrochem. Soc. 146 (1999) 4009.